2.2.2) Fosfatos marinos: fosforitas

- Génesis y características geológicas
- Yacimientos
- Producción y usos

GÉNESIS Y CARACTERÍSTICAS GEOLÓGICAS

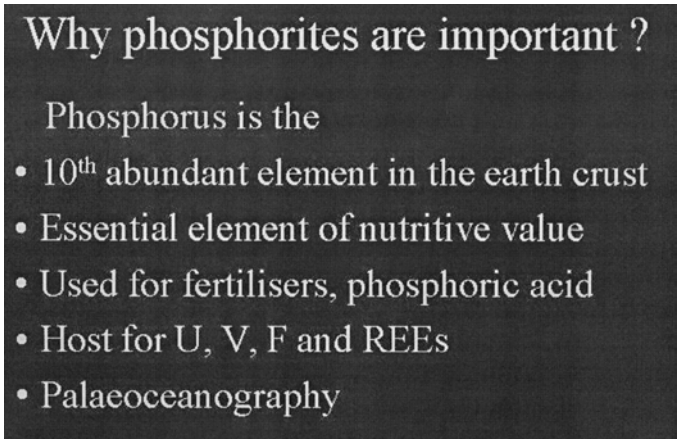

www.iac.ac.in

Tableau 1 - Analyse partielle d'un os de bovin dégraissé et de l'émail d'une dent humaine, d'après Mc Connel (1973).

% pondéral	Os	Email
P_2O_5	28,58	39,90
CaO	37,56	50,93
MgO	0,72	0,35
Na_2O	0,99	0,94
K_2O	0,07	0,037
SiO_2	0,04	0,01
CO_2	3,48	2,08
F	0,07	
Cl	0,08	0,32
Perte à 68°		2,12
Perte à 500°		2,80

M. Slansky(1980): Géologie des phosphates sédimentaires. Mem. BRGM, 114, 92 pp.

Table 127 Chemistry of Commercial Phosphate Concentrates (%)

	Jordan 70/72% TCP Sed.	USA Florida 77% BPL Sed.	USA Idaho Sed.	Morocco Youss-oufiaun Sed.	Finland Siilinjärvi Igneous	Brazil Fosfago Igneous	Nauru calcined Guano
P_2O_5	32.5	35.31	32.3	34.14	35.3	36.73	39.92
CaO	50.00	50.10	45.85	53.84	NA	49.21	54.42
CO_2	4.7	2.98	2.1	2.9	6.9	0.58	2.04
MgO	0.45	0.23	0.17	0.46	1.3	0.06	-
K_2O	0.03	0.08	0.61	0.09	0.04	0.005	trace
Na_2O	0.45	0.4	0.46	0.89	0.1	0.002	0.45
Al_2O_3	0.5	1.02	2.13	0.33	0.2	0.26	
Fe_2O_3	0.35	1.03	0.95	0.15	0.5	2.55	
SiO_2	5.35	3.05	9.87	2.72	0.5	1.42	0.4
F	3.65	3.87	2.99	4.25	2.5	2.47	2.62

Harben y Kuzvart (1996)

Distribution of Phosphorus

- Continental sediments and soils 0.15% P_2O_5
- Igneous rocks 0.07%
- Marine sediments 0.2%
- Organisms

Diatoms – 0.3 –1.27% (on dry weight)

Echinoderms – 0.8%; Green algae – 2.7%

Phytoplankton – 0.3-0.5%; Fishes – 0.9-1.83%

www.iac.ac.in

Dissolved phosphorus (P) in marine waters

Dissolved P (µg/l)	Surface layers	Interm. layers	Deeper layers
Inorganic P	0.1-40	100	100-140
Organic P	6-60	40-60	40-70

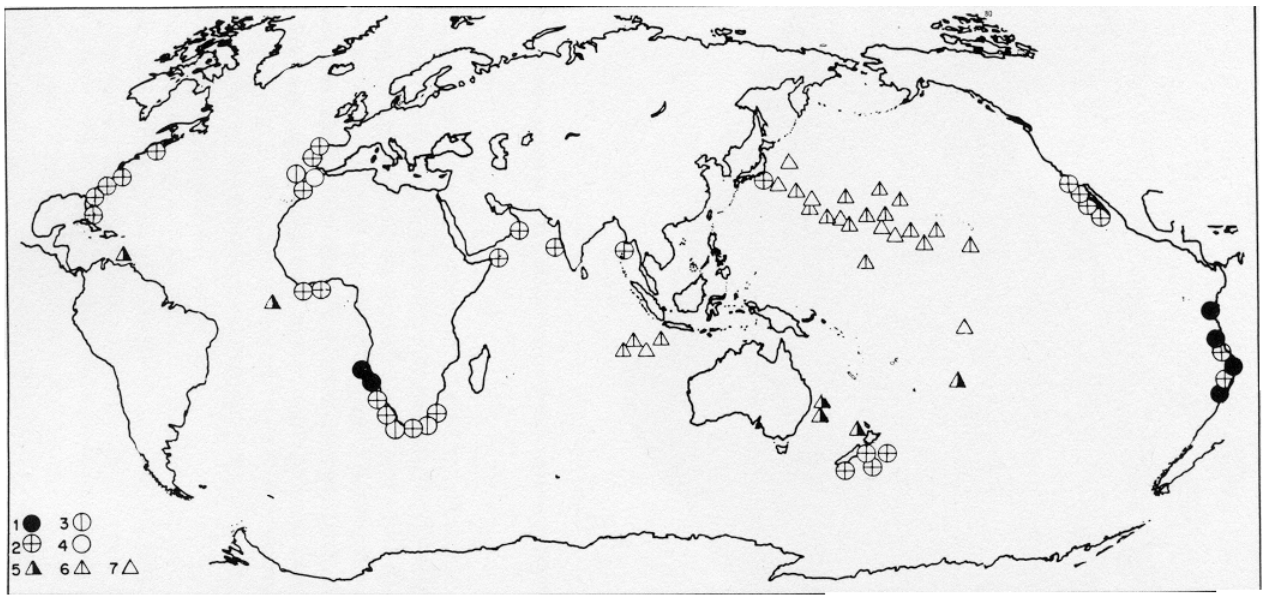

Fig. 16. Phosphorite location on the sea floor. 1–4 = phosphorites on continental margins; 5–7 = phosphorites on submerged mo
Geological age: 1 = Holocene; 2–5 = Neogene; 3–6 = Paleogene; 4, 7 = Cretaceous (from Bezrukov and Baturin, 1979).

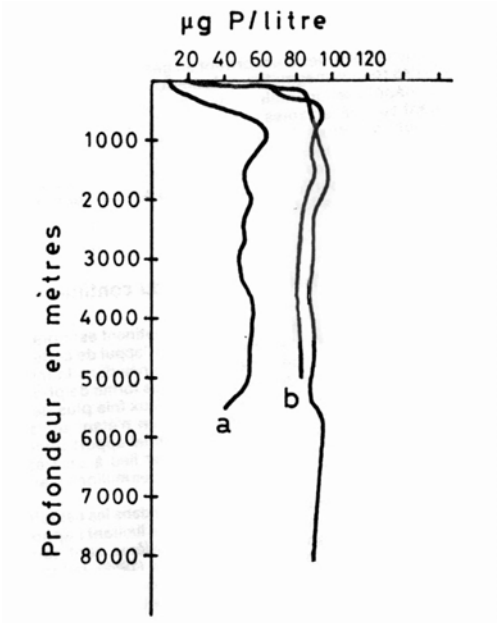

Figure 8 - Variation des teneurs en phosphore minéral dissous en fonction de la profondeur, a - Atlantique nord ; b - Océan Indien ; c Pacifique nord.

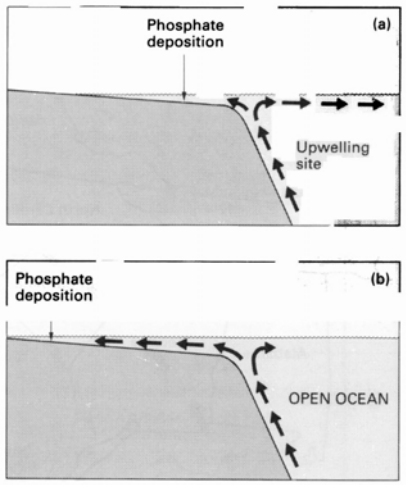

Fig. 20.8 Possible model for phosphorite formation beside an upwelling site initiated in a deep ocean. (a) Nutrient-rich, deep ocean water floods on to the continental shelf and low grade phosphorite deposits form. (b) A sea level rise leads to a major marine transgression resulting in reworking of phosphatic shelf sediments and the shoreward transport of phosphatic grains to form major deposits in the coastal zone and in marginal embayments. (After Cook 1984.)

M. Slansky (1980)

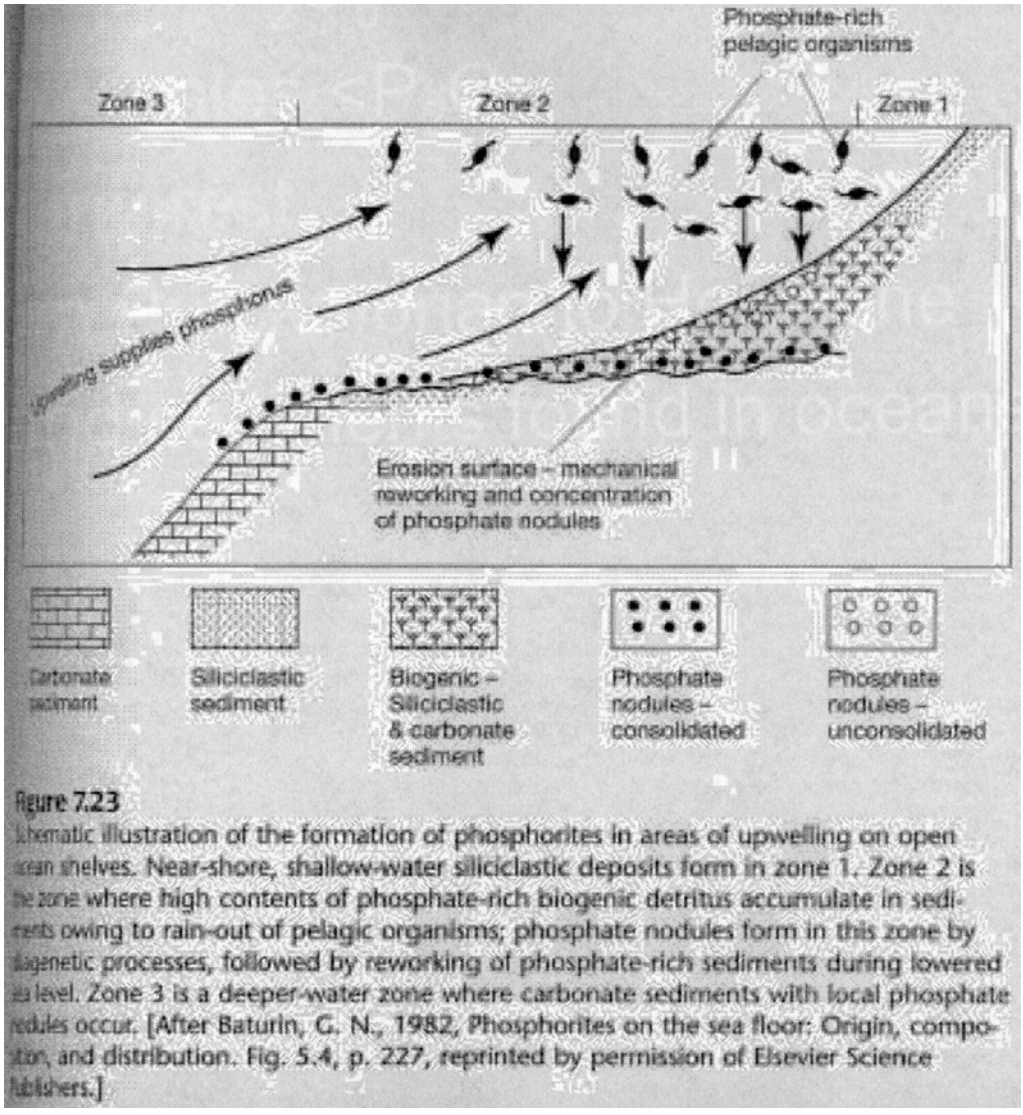

Figure 7.23
Schematic illustration of the formation of phosphorites in areas of upwelling on open ocean shelves. Near-shore, shallow-water siliciclastic deposits form in zone 1. Zone 2 is the zone where high contents of phosphate-rich biogenic detritus accumulate in sediments owing to rain-out of pelagic organisms; phosphate nodules form in this zone by diagenetic processes, followed by reworking of phosphate-rich sediments during lowered sea level. Zone 3 is a deeper-water zone where carbonate sediments with local phosphate nodules occur. [After Baturin, G. N., 1982, Phosphorites on the sea floor: Origin, composition, and distribution. Fig. 5.4, p. 227, reprinted by permission of Elsevier Science Publishers.]

TABLE II. Distribution of known Miocene sediments containing phosphorites along the modern continental margins.

CONTINENTAL MARGIN	REGION
East Atlantic:	Portugal, Northwest Africa through South Africa, and Agulhas Bank
West Atlantic	North Carolina through Florida, Cuba, Venezuela, and Argentina
East Pacific:	California through Baja California, Mexico, and Peru through Chile
West Pacific:	Sakalin Island, Sea of Japan, Indonesia, Chatham Rise east of New Zealand, and East Australian shelf.

Teleki et al. (edt) 1987

— **42.** Nodules à 25 à 30 % P_2O_5 du Dinantien des Pyrénées. Le nodule scié de gauche laisse apparaître une structure concentrique, soulignée par les variations de concentration de la matière organique. La pièce de 1 F donne l'échelle.

— **43.** Nodules de l'Albien du NE du Bassin de Paris à teneur en P_2O_5 variable (5 à 25 %) et formes diverses, souvent très irrégulières. Certains sont des moules internes de Lamellibranches, Gastéropodes ou Ammonites.

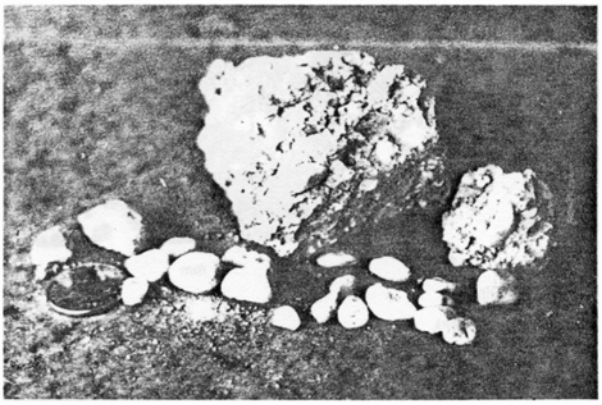

— **44.** « Pebbles » de la formation phosphatée miopliocène de Floride. Pour S.R. Riggs (1979) ces galets sont des intraclastes. Ils contiennent souvent du quartz et leur teneur (30 à 32 % P_2O_5) est généralement inférieure à celle des pellets.

M. Slansky (1980)

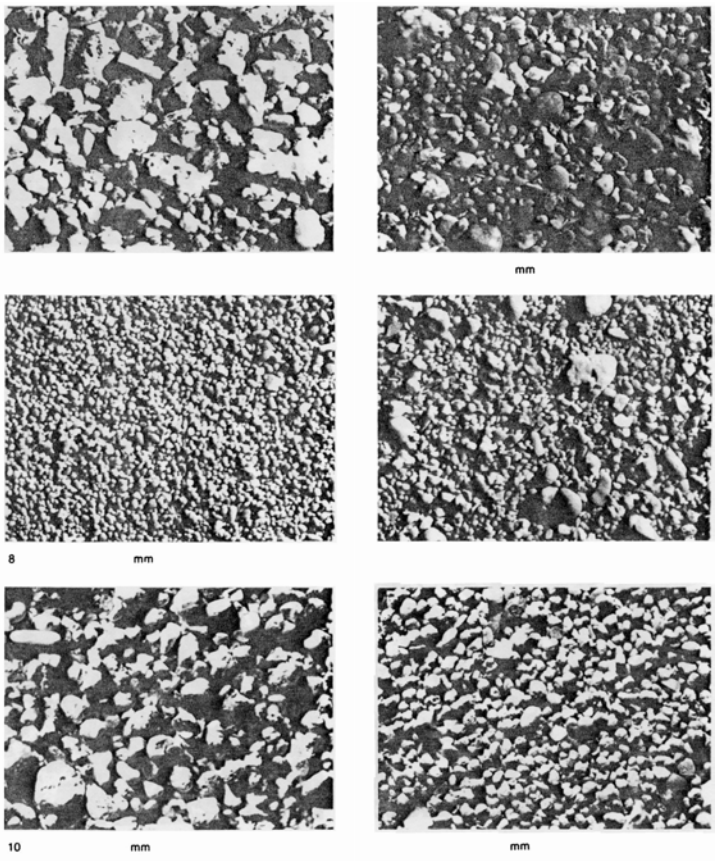

Morphologie des grains des phospharénites :

— **6.** Sénonien d'Égypte (vallée du Nil) — **7.** Sénonien d'Arabie saoudite (West Thanyat) — **8.** Paléocène du Maroc (Bou aa) — **9.** Éocène moyen du Bénin (Lokossa) — **10.** Éocène moyen du Sénégal (Taïba) — **11.** Miocène de Californie (Indian Creek).

M. Slansky (1980)

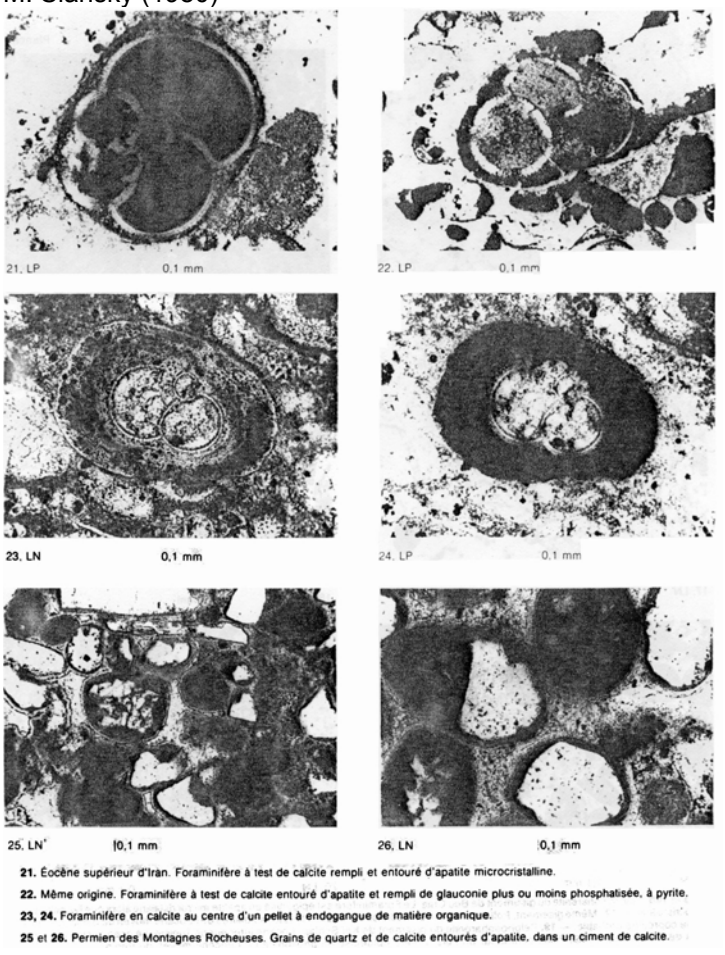

21. Éocène supérieur d'Iran. Foraminifère à test de calcite rempli et entouré d'apatite microcristalline.

22. Même origine. Foraminifère à test de calcite entouré d'apatite et rempli de glauconie plus ou moins phosphatisée, à pyrite.

23, 24. Foraminifère en calcite au centre d'un pellet à endogangue de matière organique.

25 et **26.** Permien des Montagnes Rocheuses. Grains de quartz et de calcite entourés d'apatite, dans un ciment de calcite.

Tableau 6 - Subdivisions de la classe des rudites.

Termes français	Termes anglo-saxons
2 mm	
granule	granule
4 mm	
gravier	
16 mm	pebble
galet	
64 mm	
petit bloc	cobble
256 mm	
bloc	boulder

M. Slansky (1980)

Tableau 7 - Principales classes de phosphatites.

Fraction phosphatée principale \ Exogangue	Siliceuse clastique >10 µm	Chartreuse <10 µm	Argilo-marneuse	Carbonatée	Autres
Microsphatite					
Phosphalutite					
Phosphorénite					
Phosphorudite					

Teleki et al. (edt) 1987

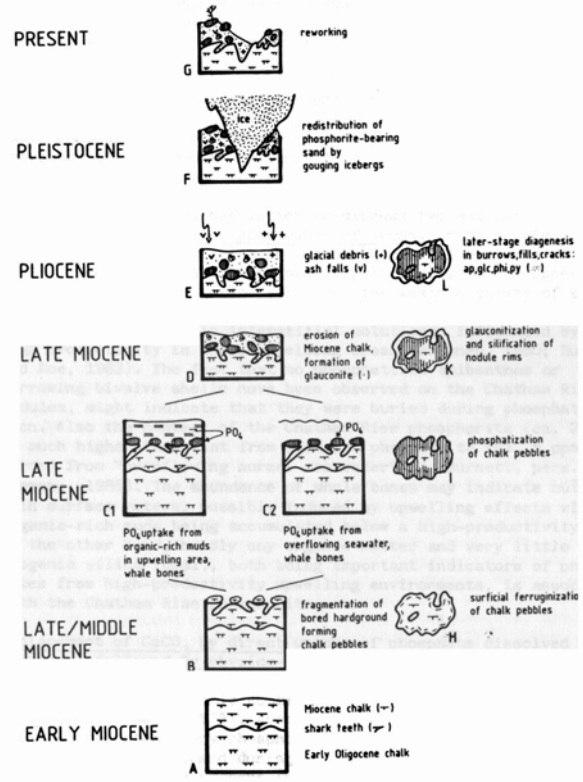

Fig. 7. Schematic sketch showing Neogene evolution, genesis and diagenesis of phosphorite and associated sediment on the central Chatham Rise (C_1 and C_2 are alternative models for phosphatization process, see text). Evolution of chalk pebbles to phosphorite nodules is shown in four steps. From Kudrass and von Rad (1984b).

Table 126 Phosphate Minerals

Minerals	Formula	Color/Luster	SG	H	Crystal system/ habit	Occurrences
Brushite George Jarvis Brush (1831-1912), mineralogist, Yale U	$CaHPO_4 \cdot 2H_2O$	colorless to ivory yellow; transparent to translucent; vitreous	2.26 - 2.33	2½	monoclinic; needlelike, prismatic, or tabulat xls; earthy or powdery	guano such as in cave near Oran, Algeria, on Aves Island in the Caribbean
Chlorapatite Greek *apate = deceit* since it was often mistaken for other minerals plus Cl	$Ca_5(PO_4)_3Cl$ 41% P 6.8 % Cl *a.k.a. Francolite*	pinkish, white, pale yellow; transparent to translucent; vitreous	3.1 - 3.2	5	trigonal, monoclinic; short to long prismatic xls	calc-silicate marbles assoc. with actinolite, diopside; in veins in gabbroic rocks; as microgranules in meteorites
Crandallite (pseudowavellite) Milan L. Crandell Jr., American engineer, Provo, Utah	$CaAl_3(PO_4)_2(OH)_5 \cdot H_2O$	yellow to yellowish white to white or gray; transparent to subtranslucent; vitreous	2.78 - 2.92	5	triclinic, trigonal; minute xls or rosettes of fibers; massive, nodular or spherulitic	assoc. with rare secondary phosphate minerals in variscite nodules, and with barite and quartz
Fluorapatite containing fluorine and apatite	$Ca_5(PO_4,CO_3,OH)_3(F,OH)$ 42.3% P 3.8% F	colorless, white, gray, yellow to yellowish green, bluish green, blue, violet, purple; transparent - opaque; vitreous - subresinous; fluorescent, phosphorescent	3.1 - 3.2	5	trigonal; short to long prismatic xls, thin to thick tabular, massive, compact, coarse granular; globular or reniform; stalactitic; fibrous	igneous rocks; hydrothermal and Alpine-type veins; as bedded deposits of marine origin; metamorphic rocks; detrital deposits
Millisite for F.T. Mills, of Lehi, Utah, the first observer	$(Na,K)CaAl_6(PO_4)_4(OH)_9 \cdot H_2O$	white, light gray, greenish	2.83 - 2.87	5½	tetragonal; as chalcedonic crusts or spherules with finely fibrous structure	in aluminous phosphate zone of Bone Valley Formation in FL in USA; in Senegal deposits
Monetite locality of Island of Moneta, Caribbean Sea	$(CaHPO_4)$	colorless, white, pale yellow; transparent to translucent; vitreous	2.92	3½	triclinic; massive aggregates of minute flattened xls with rough faces	on islands in Caribbean and South Atlantic; cave deposits
Wavellite William Wavell (d.1829), physician, Horwood Parish, Devon, UK	$Al_3(PO_4)_2(OH)_3 \cdot 5H_2O$	white to greenish, yellow, yellowish brown or green, brown to brownish black; transparent - translucent; vitreous - resinous or pearly	2.36 - 2.37	3½ - 4	orthorhombic; acicular radiating aggregates, as crusts, stalactitic	secondary mineral in hydrothermal veins; certain Al metamorphic rocks; phosphate-rock and limonite deposits

Source: various including Roberts et al., 1990

Harben y Kuzvart (1996)

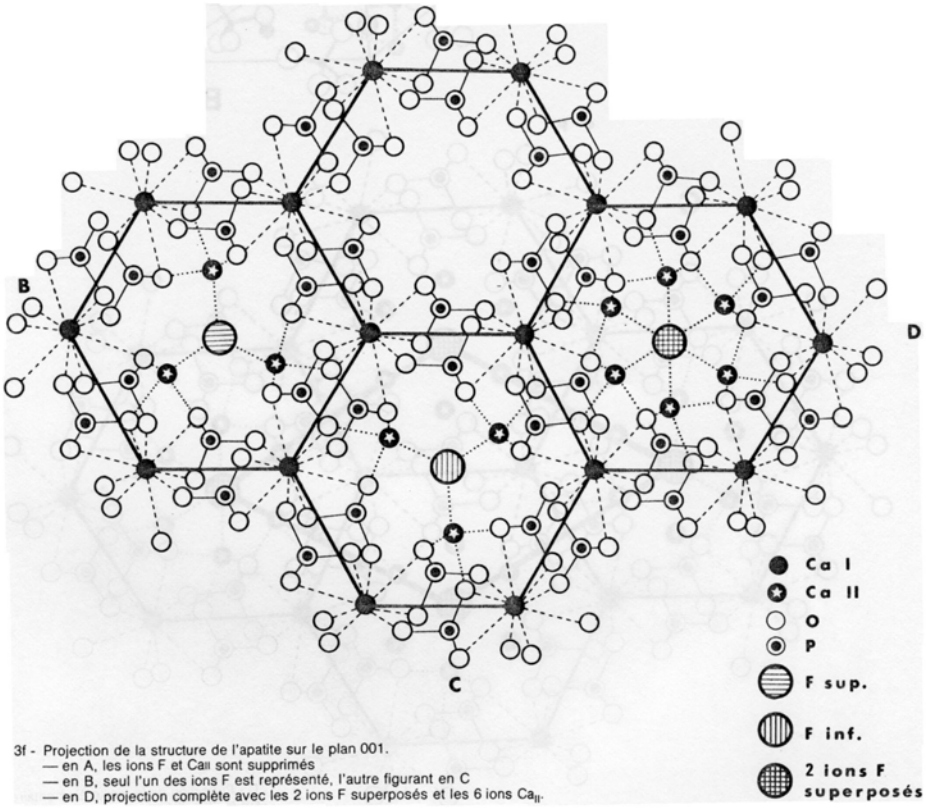

3f - Projection de la structure de l'apatite sur le plan 001.
— en A, les ions F et Ca_{II} sont supprimés
— en B, seul l'un des ions F est représenté, l'autre figurant en C
— en D, projection complète avec les 2 ions F superposés et les 6 ions Ca_{II}.

M. Slansky (1980)

Table 1. Some possible substitutions in the apatite structure

Constituent ion	Substituting ion
Ca^{2+}	Na^{+}, K^{+}, Ag^{+} Sr^{2+}, Mn^{2+}, Mg^{2+}, Zn^{2+}, Cd^{2+}, Ba^{2+} Sc^{3+}, Y^{3+}, R. E.$^{3+}$ (rare earths), Bi^{3+} U^{4+}
PO_4^{3-}	CO_3^{2-}, SO_4^{2-}, CrO_4^{2-} AsO_4^{3-}, VO_4^{3-}, $CO_3 \cdot F^{3-}$, $CO_3 \cdot OH^{3-}$ SiO_4^{4-}
F^{1-}	OH^{1-}, Cl^{1-}, Br^{1-} O^{2-}

Nriagu y Moore (edts) (1984): Phosphate Minerals. Ed. Springer-Verlag, 435 pp

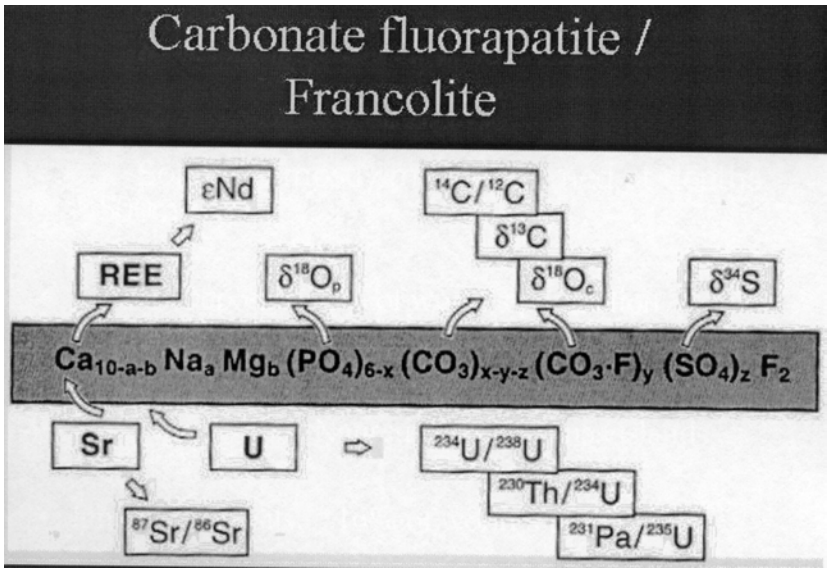

www.iac.ac.in

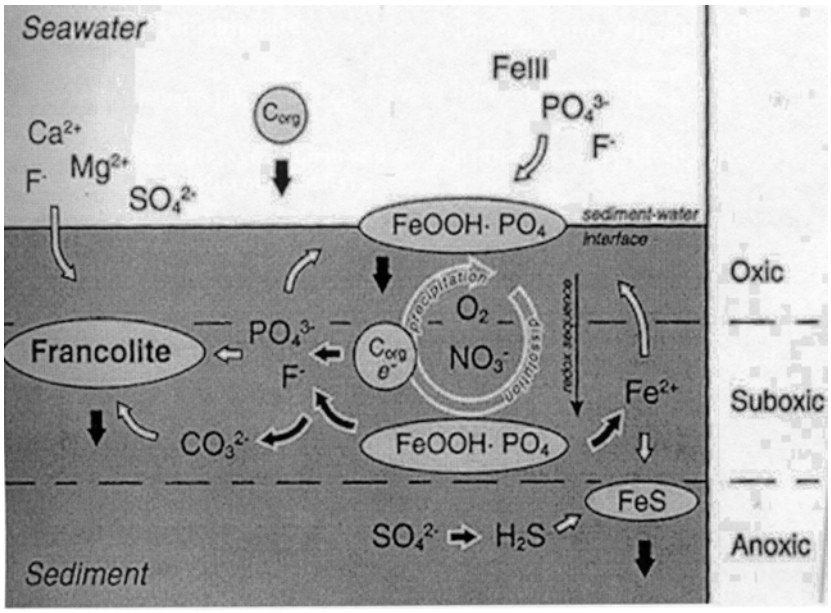

YACIMIENTOS

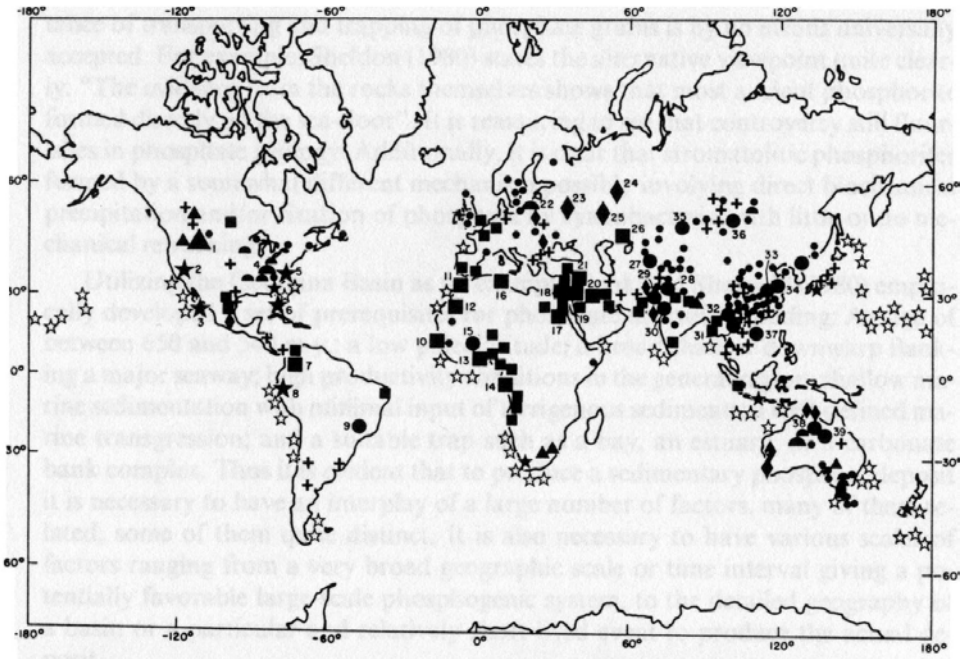

Fig. 3. Distribution of sedimentary phosphate deposits and occurrences. Major deposits are numbered as follows: *1* Phosphoria, USA; *2* Monterey, USA; *3* Baja California, Mexico; *4* Tennessee, USA; *5* N Carolina, USA; *6* Florida, USA; *7* Cordillera, Colombia; *8* Sechura, Peru; *9* Bambui, Brazil; *10* Taiba, Senegal; *11* Khourigba etc, Morocco; *12* Bu Craa, Morocco; *13* Hahotoe, Togo; *14* Cabinda; *15* Volta and Niger; *16* Gafsa, Tunisia and Djebel Onk, Algeria; *17* Abu Tatur, Egypt; *18* Machtesh area, Israel; *19* El Hassa, Jordan; *20* Iraq; *21* Palmyra, Syria; *22* Maadu, USSR; *23* Moscow Basin, USSR; *24* Yegorevsk, USSR; *25* Rudnichny, USSR; *26* Aktyubinsk, USSR; *27* Karatau, USSR; *28* Maldeota, India; *29* Hazara, Pakistan; *30* Rajasthan, India; *31* Laokoy, Vietnam; *32* Kunming, China; *33* Kaiyang, China; *34* Xingyang, China; *35* Abaka, USSR; *36* Hubsugul, Mongolian People's Republic; *37* Hainan, China; *38* Alexandria-Wonarah (NT), Australia; *39* Duchess etc (Qld), Australia

Nriagu y Moore (edts) (1984)

Ancient Phosphorites	Modern/Quat. Phosphorites
• Grainstone phosphorites	Phosphorite nodules
• **Stromatolites (stratiform and columnar Microbial mats)**	Stromatolites are unknown
• A few meters to 100 m thick Phosphorite beds	Scattered on the sea floor
• Both upwelling and non-upwelling regions	Mostly confined to the western margins - **upwelling regions**
• Extensive reworking & **Benthic microbial activity**	**Inorganic processes**

No Modern/Quat. analogs for ancient phosphorites - (Bentor, 1980; Cook, 1994) ??

www.iac.ac.in

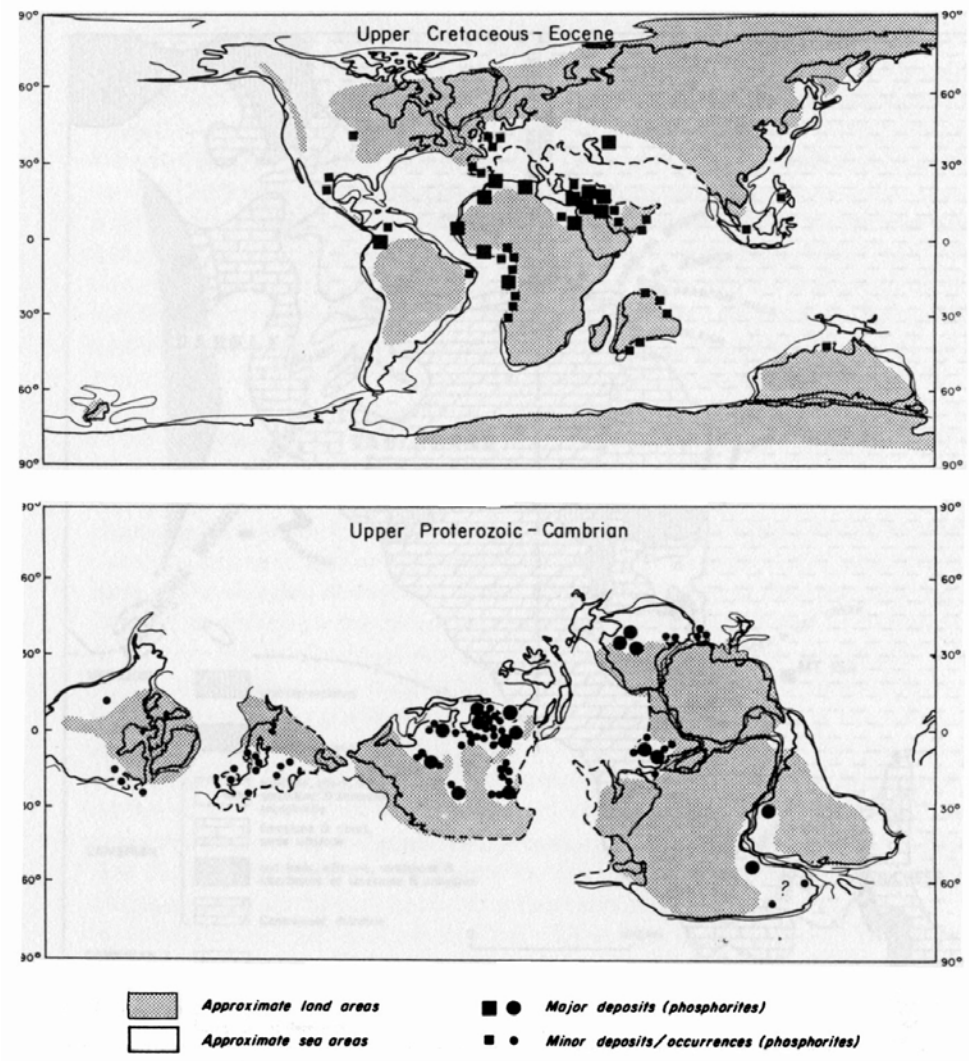

Fig. 4. Distribution of phosphorites. The reconstruction for the upper Cretaceous-Eocene utilizes a Santonian reconstruction, the Upper Proterozoic-Cambrian utilizes an Aldian reconstruction. Both reconstructions are after Smith et al. (1981) and are based on cylindrical equidistant projection

Nriagu y Moore (edts) (1984)

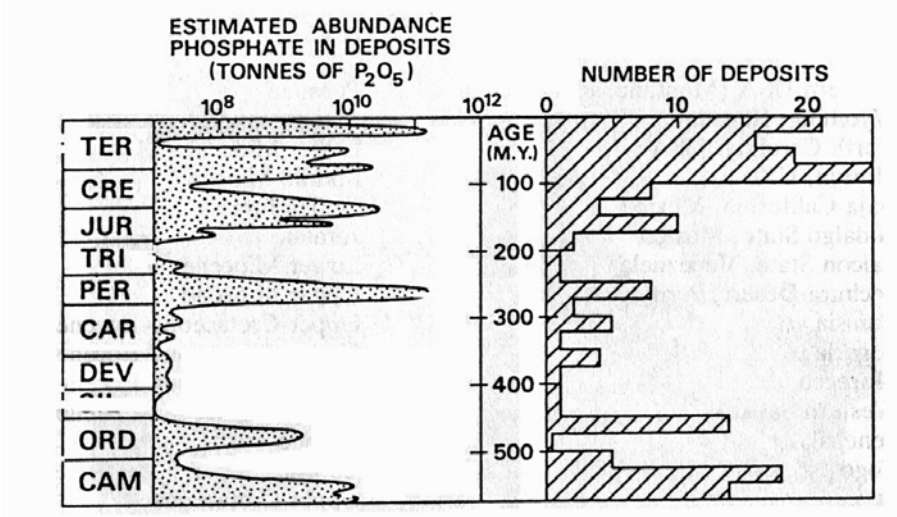

Figure 4.8 Temporal distribution of phosphate deposits (from Cook, 1984).

Table 1. Major phosphogenic episodes. (After Cook and McElhinny 1979)

Episode	Mean age (m.y.)	Locations
Miocene-Pliocene	14	Continental margins; *SE USA*[a], California, *Sechura*, Venezuela, Japan, Philippines
Upper Cretaceous-Eocene	65 { 54[b] 77[b]	*W Africa*, *N Africa*, *Mid East*, W Europe, N South America, Mexico, N India, Ukraine, Kazakhstan, W Australia, Pakistan, Texas, Manitoba
Jurassic	149	*Russia*, Mexico, N South America, W Europe, W Australia, N India, Pakistan, W Canada
Permian	250	*W USA*, Urals, Szechwan, Indochina, N India
Ordovician	464	*Tennessee*, Ala., Ken., Central and SE Australia, *Baltic area*, Iowa, E Canada, Bolivia, Baikal
Cambrian	542	*Karatau*, *Russia*, *Georgina Basin*, *Central and SE China*, *Vietnam*, *Hubsugul*, S Australia, Tien Shan, Sayan, Central Kazakhstan, Tennessee, E Canada, Mauritania
Upper Proterozoic I	620	*Volta area*, Mauritania, China(?)
Upper Proterozoic II	700– 800	*China*, Central Siberia, India(?), Brazil, Central Australia
Middle Proterozoic(?)	1,200–1,600	Yenisei, *Rajasthan*(?)
Lower Proterozoic	1,800–2,200	Rum Jungle, Broken Hill, Australia(?), Michigan, Finland

[a] Regions with very large deposits are italicized
[b] Secondary peaks may be present at about these times

Nriagu y Moore (edts) (1984)

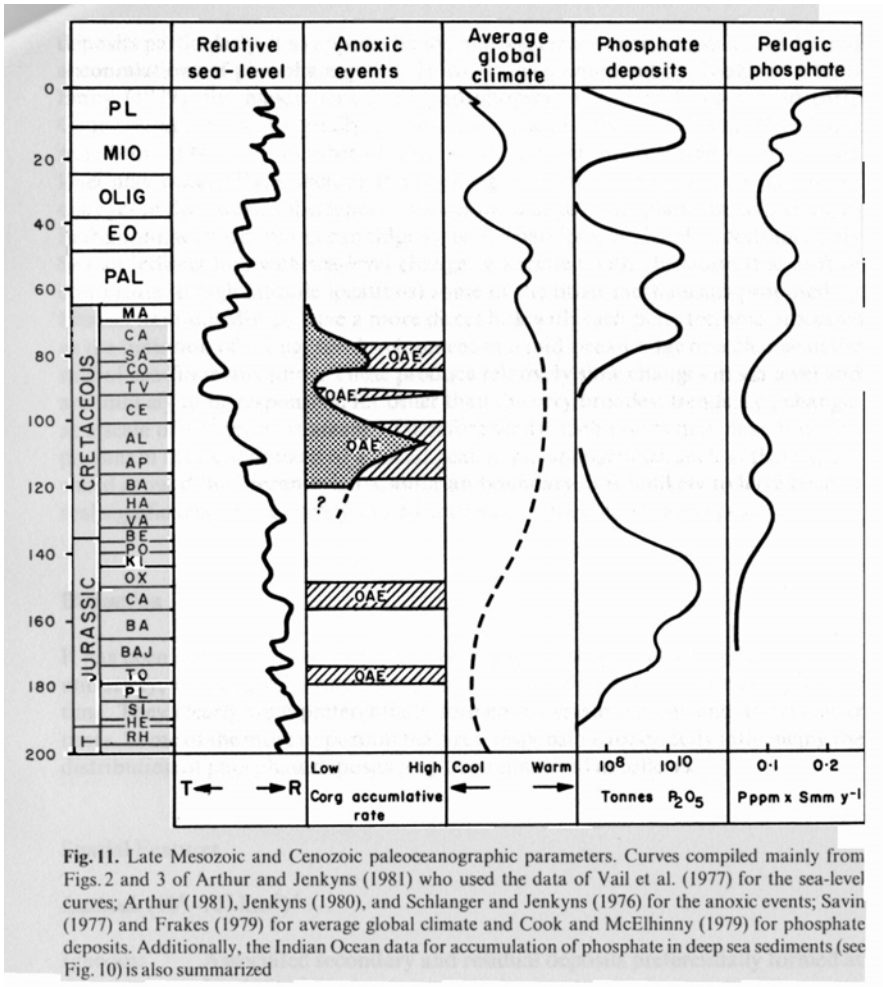

Fig. 11. Late Mesozoic and Cenozoic paleoceanographic parameters. Curves compiled mainly from Figs. 2 and 3 of Arthur and Jenkyns (1981) who used the data of Vail et al. (1977) for the sea-level curves; Arthur (1981), Jenkyns (1980), and Schlanger and Jenkyns (1976) for the anoxic events; Savin (1977) and Frakes (1979) for average global climate and Cook and McElhinny (1979) for phosphate deposits. Additionally, the Indian Ocean data for accumulation of phosphate in deep sea sediments (see Fig. 10) is also summarized

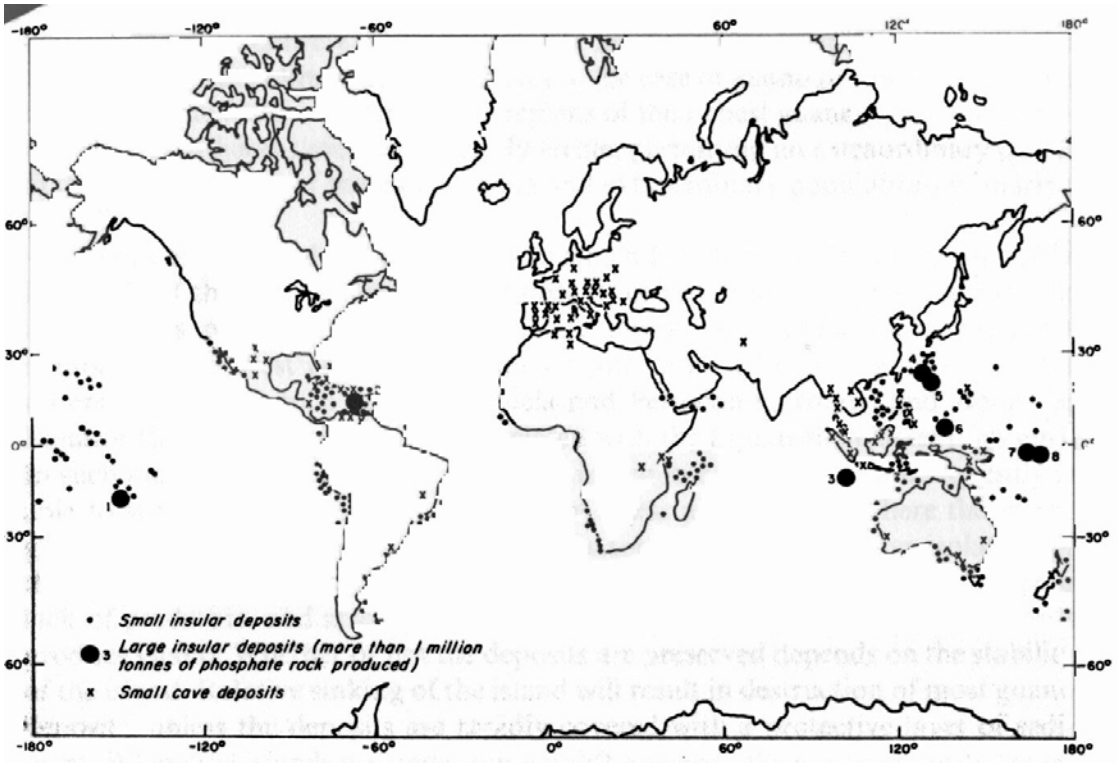

Fig. 2. Distribution of insular and cave guano deposits. Major deposits are numbered as follows: *1* Makatea, French Polynesia; *2* Curacao, Dutch Antilles; *3* Christmas Island, Indian Ocean; *4* Kita Daito Jima, NW Pacific; *5* Okino Daito Jima, NW Pacific; *6* Anguar, SW Pacific; *7* Nauru, central Pacific; *8* Ocean Island, central Pacific (now worked out)

Nriagu y Moore (edts) (1984)

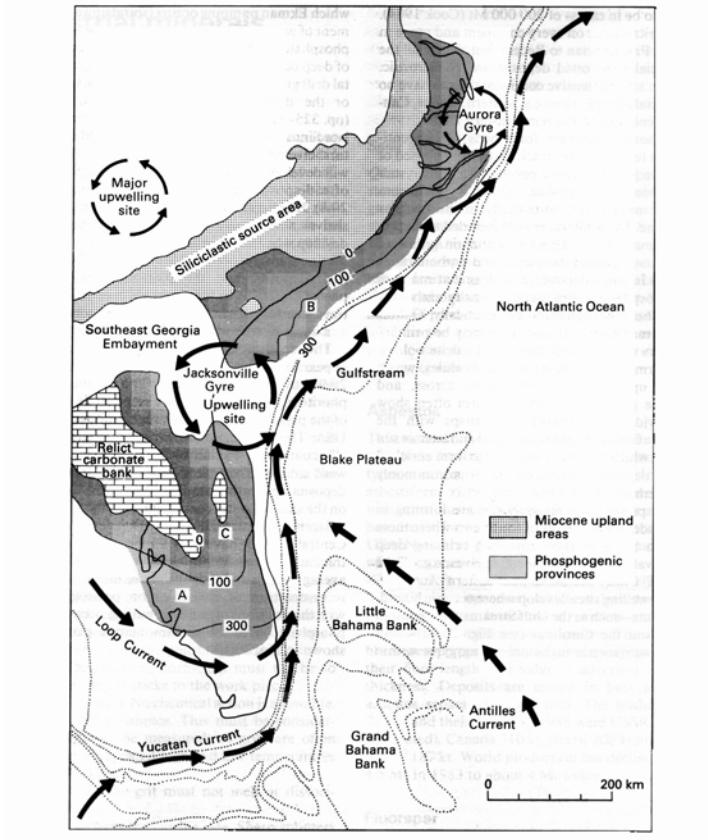

Fig. 20.10 A Miocene palaeogeographical reconstruction of the south-eastern continental margin of the USA showing oceanic currents, major topographically induced upwelling sites and areas of phosphate deposition. (After Compton *et al.* 1990, with some modifications based on van Kauwenbergh & McClellan 1990.)

Teleki et al. (edt) 1987

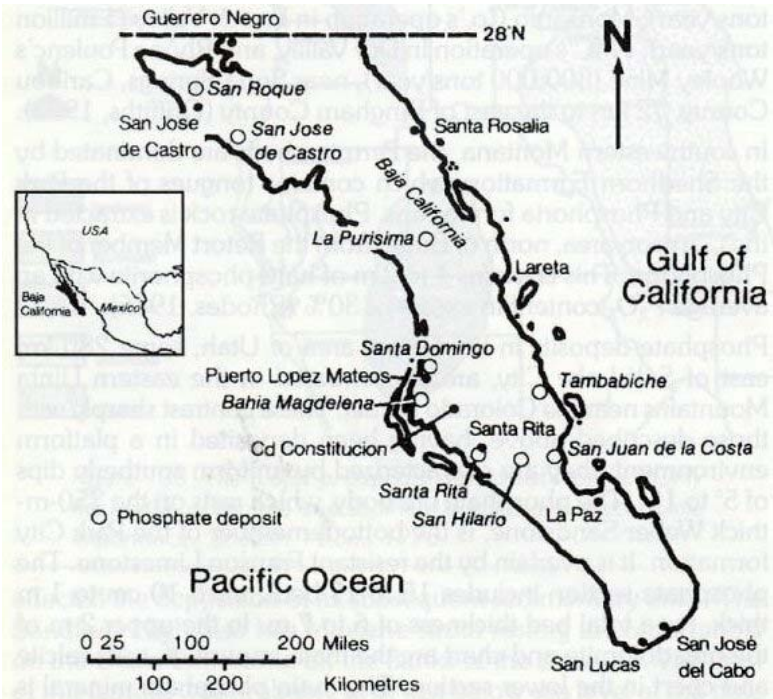

Figure 134 Phosphate occurrences and mines in the southern Baja California area of Mexico. Source: Clarke, 1980.

Harben y Kuzvart (1996)

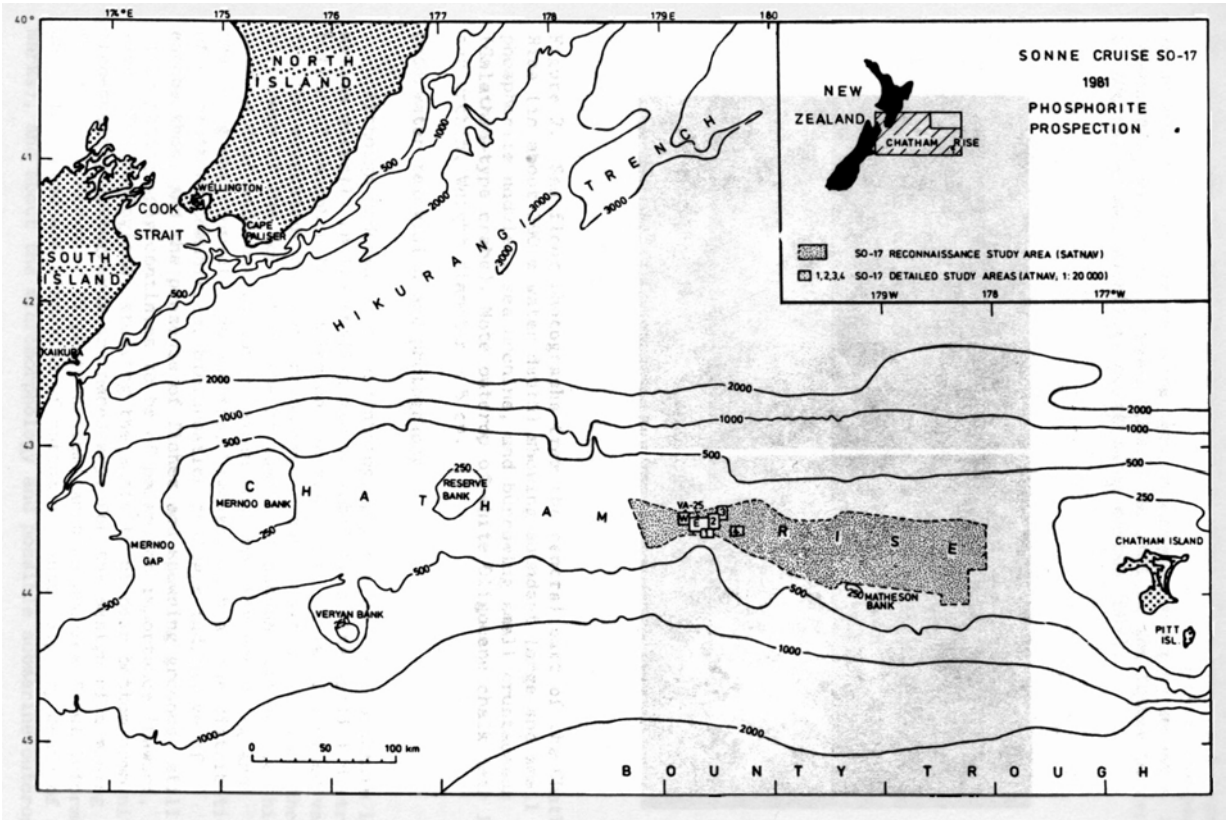

Fig. 1. Area of investigation for phosphorite deposits on the Chatham Rise (VA 25/1978 and SO-17/1981 cruises)

Teleki et al. (edt) 1987

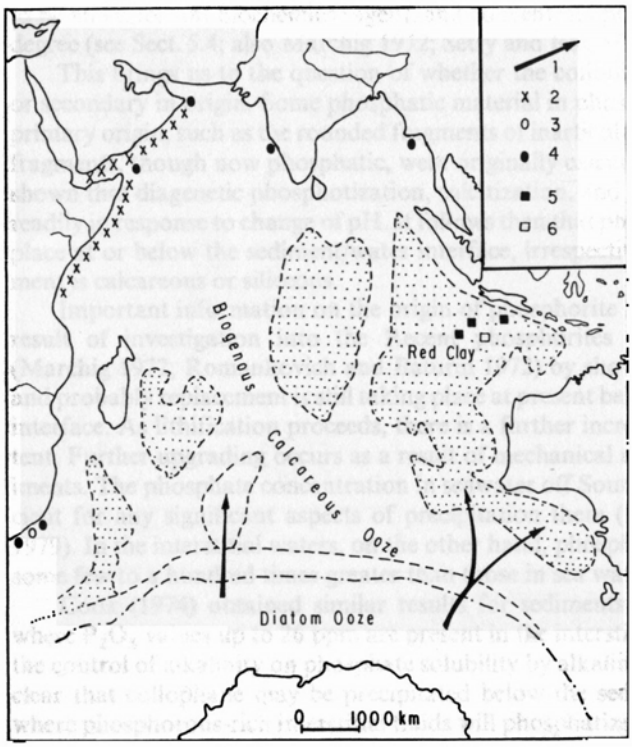

Fig. 5.2. Phosphorite locations in the Indian Ocean. Also shown are Recent deep sea sediments (*dotted*) and the zone of Antarctic convergence (*dash* - and - *dot line*). *1 (arrow)* direction of AABW entry; *2* (×) areas of upwelling; *3* (○) Paleogene phosphorites in coastal areas; *4* (●) Neogene phosphorites in coastal areas; *5* (■) Paleogene phosphorites on submerged mountains; *6* (□) Cretaceous phosphorites on submerged mountains

Teleki et al. (edt) 1987

Table I Documented examples of seamount phosphorite deposits from the Atlantic and Pacific Oceans.

Location	Reported Age	Reference
	-- ATLANTIC OCEAN --	
Aves Swell	Miocene-Holocene	Marlowe (1971)
Annan Seamount	Eocene	Jones and Goddard (1979)
New England Seamounts		Manheim (1972)
Jan Mayen Ridge		Baturin (1982)
Romanche Fracture Zone		Bonatti et al. (1970)
	-- PACIFIC OCEAN --	
Albert Henry Seamount	Late Pliocene	Cullen and Burnett (1986)
Colahan Seamount	--	Hein et al. (1985a)
Line Islands	Late Cretaceous	Haggerty et al. (1982)
		Halbach and Manheim (1984
Kalolo Seamount	--	Cullen and Burnett (1986)
Marcus-Necker Ridge	Cretaceous	Baturin (1982)
Mid-Pacific Mountains	Late Cretaceous/Eocene	Hamilton (1956)
	Pre-middle Miocene	Halbach et al. (1982)
		Halbach and Manheim (1984
		Hein et al. (1985a)
Milwaukee Bank	Neogene	Baturin (1982)
Musicians Seamounts	Miocene and older (?)	Burnett et al. (1983)
		DeCarlo et al. (1986)
Necker Ridge	--	Hein et al. (1985b)
North Fiji Plateau	--	Cullen and Burnett (1986)
Sylvania Guyot	Cretaceous	Hamilton and Rex (1959)
S.P. Lee Guyot	--	Hein et al. (1985b)
Tasman Sea Guyots	Late Pliocene/ Pleistocene	Slater and Goodwin (1973)
Wake and Geisha Seamounts	Late Cretaceous/Eocene	Heezen et al. (1973)

Exploración de fosforitas

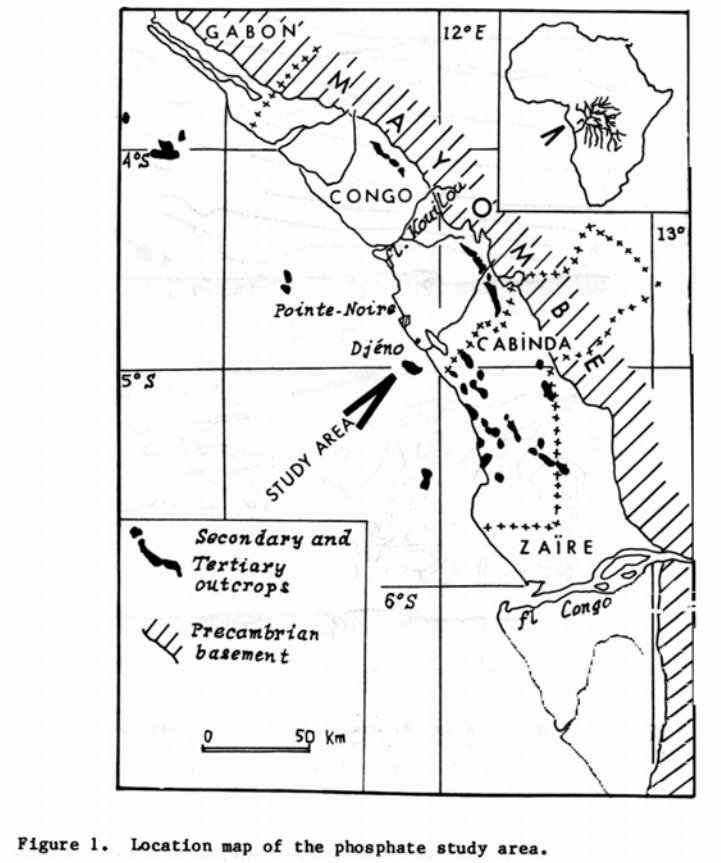

Figure 1. Location map of the phosphate study area.

Teleki et al. (edt) 1987

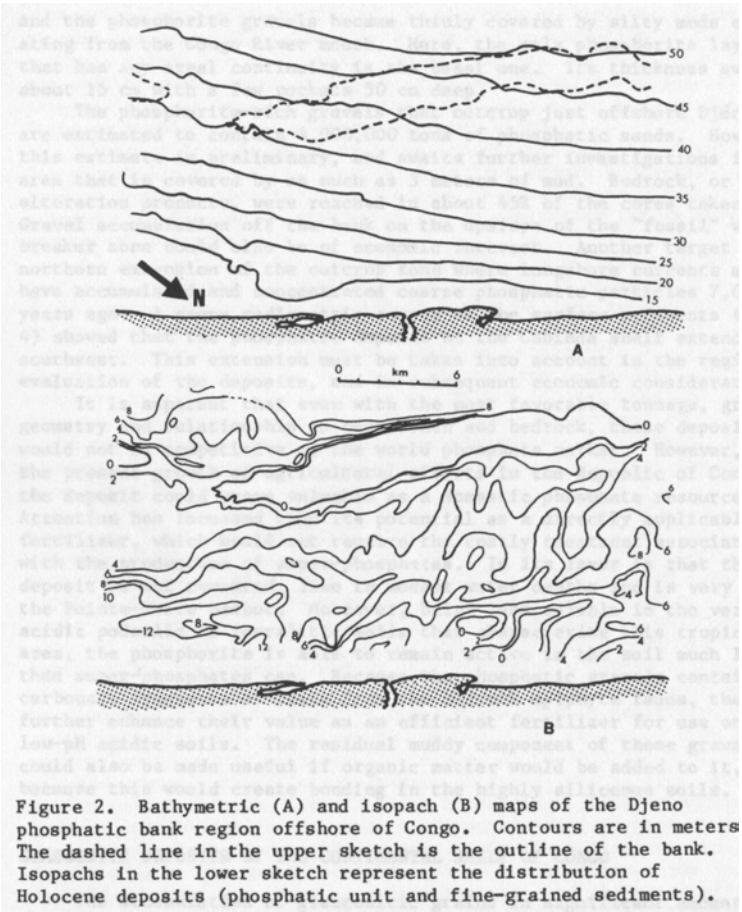

Figure 2. Bathymetric (A) and isopach (B) maps of the Djeno phosphatic bank region offshore of Congo. Contours are in meters The dashed line in the upper sketch is the outline of the bank. Isopachs in the lower sketch represent the distribution of Holocene deposits (phosphatic unit and fine-grained sediments).

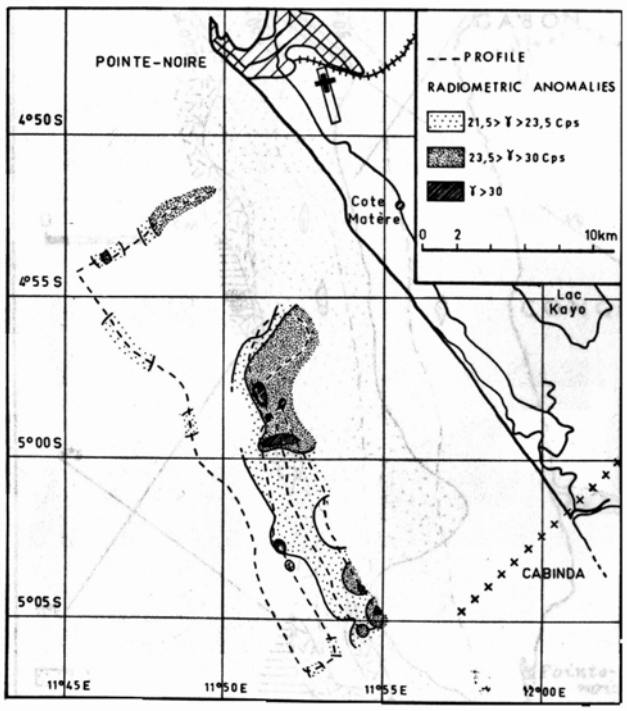

Figure 4. Distribution of phosphatic sediments as measured by gamma-ray. Values are given in counts per second (Cps).

Teleki et al. (edt) 1987

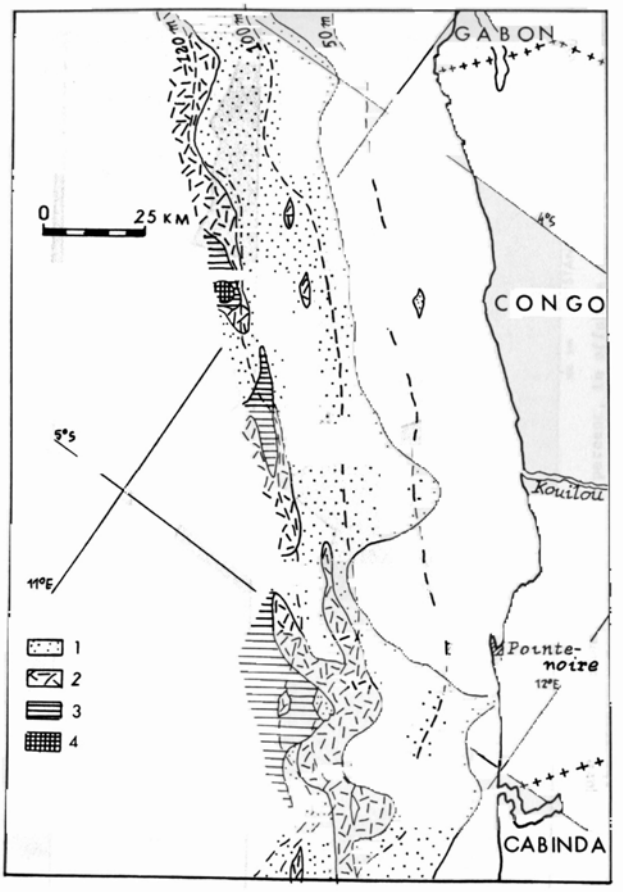

Figure 5. Distribution of the magnetic fraction in the surficial sediments of the shelf offshore of Congo. 1: 5-25%, 2: 25-75%, 3: 50-75%, 4: more than 75%.

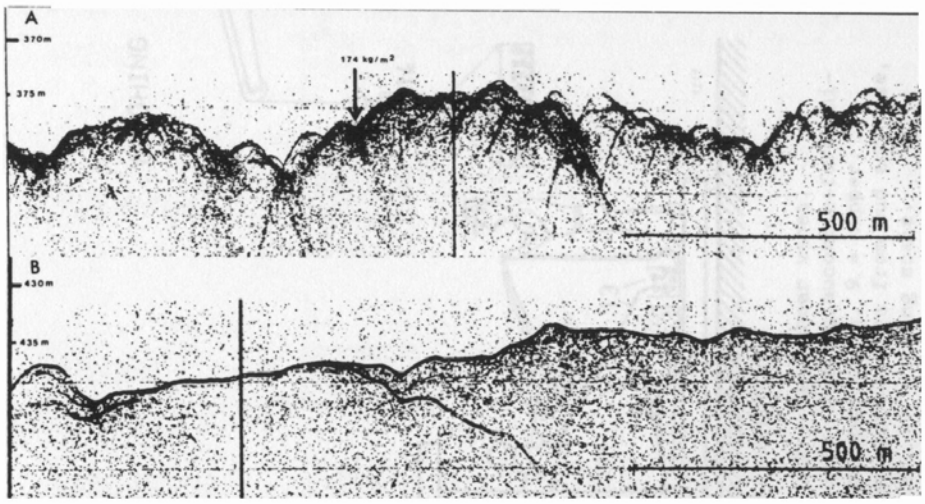

Figure 4. Correlation of high-resolution seismic (boomer) record with phosphorite yield (kg/m²).
A. Continuous overlapping diffraction hyperbolae with hummocky surface (high to intermediate relief), without bottom reflector. Samples from this "seismic facies type" have usually a high phosphorite yield.
B. Smooth to irregular, rolling bottom topography without diffraction hyperbolae, but with distinct subbottom reflectors. Usually, no phosphorite was found in areas with this "seismic facies".

Teleki et al. (edt) 1987

Explotación de fosforitas

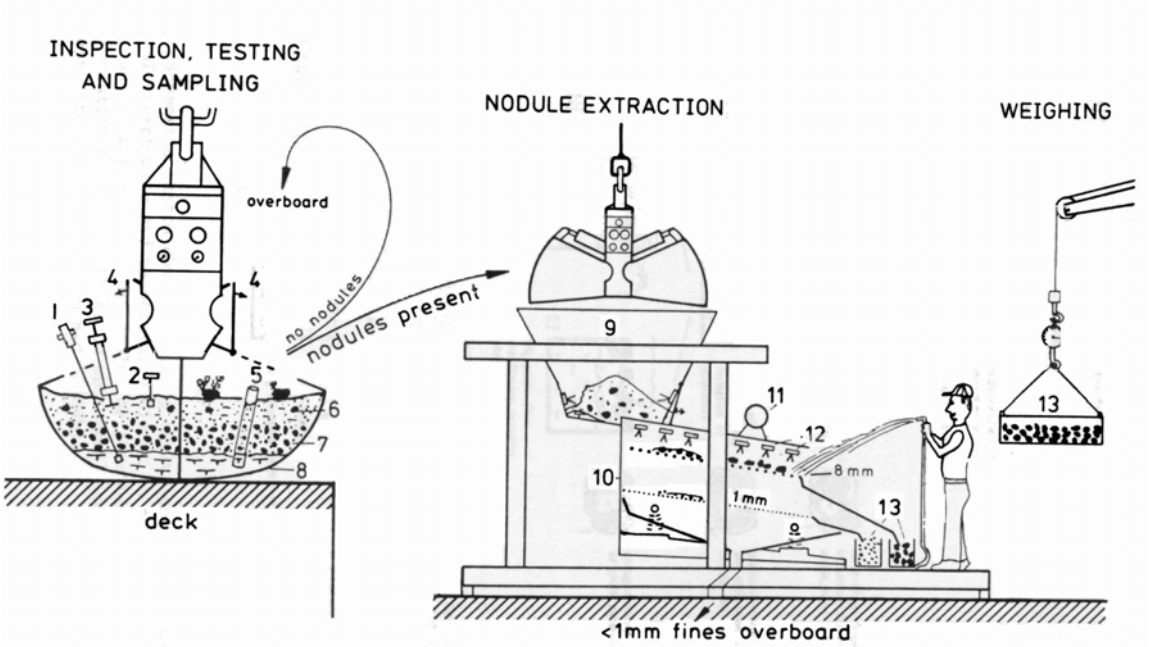

Fig. 6. Sketch of shipboard processing of large grab sampler. 1,2 = hand shear vanes, 3 = plate-bearing test, 4 = grab doors, 5 = sampling tube, 6 = soft, muddy glauconite-foraminiferal sand, 7 = same, with phosphorite nodules, 8 = nannoplankton ooze/chalk, 9 = hopper, 10 = sieve shaker, 11 = vibrating motor, 12 = water jets to wash nodules free from mud and ooze, 13 = rectangular containers for nodule fractions >8 mm and 1-8 mm, 14 = spring scale.

Teleki et al. (edt) 1987

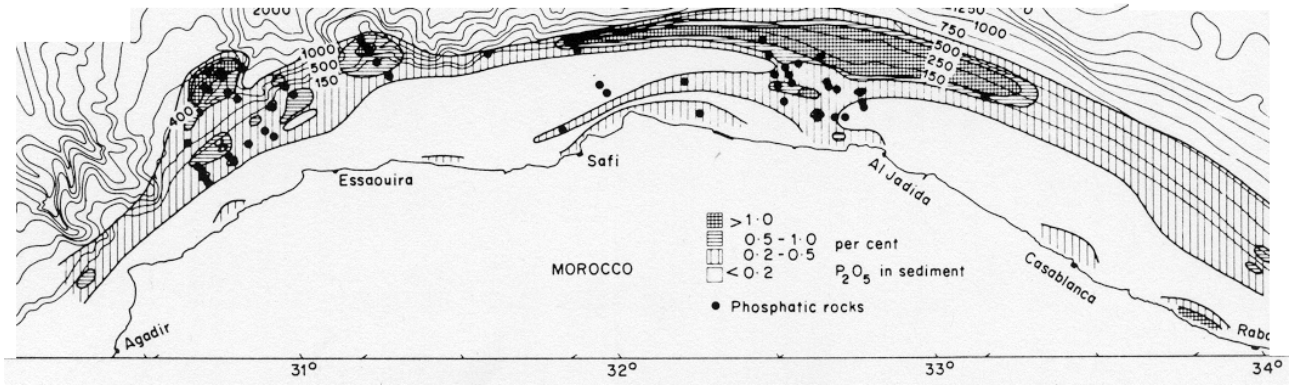

Margen continental de Marruecos con depósitos fosfatados actuales (Cook y Serhgold, 1986)

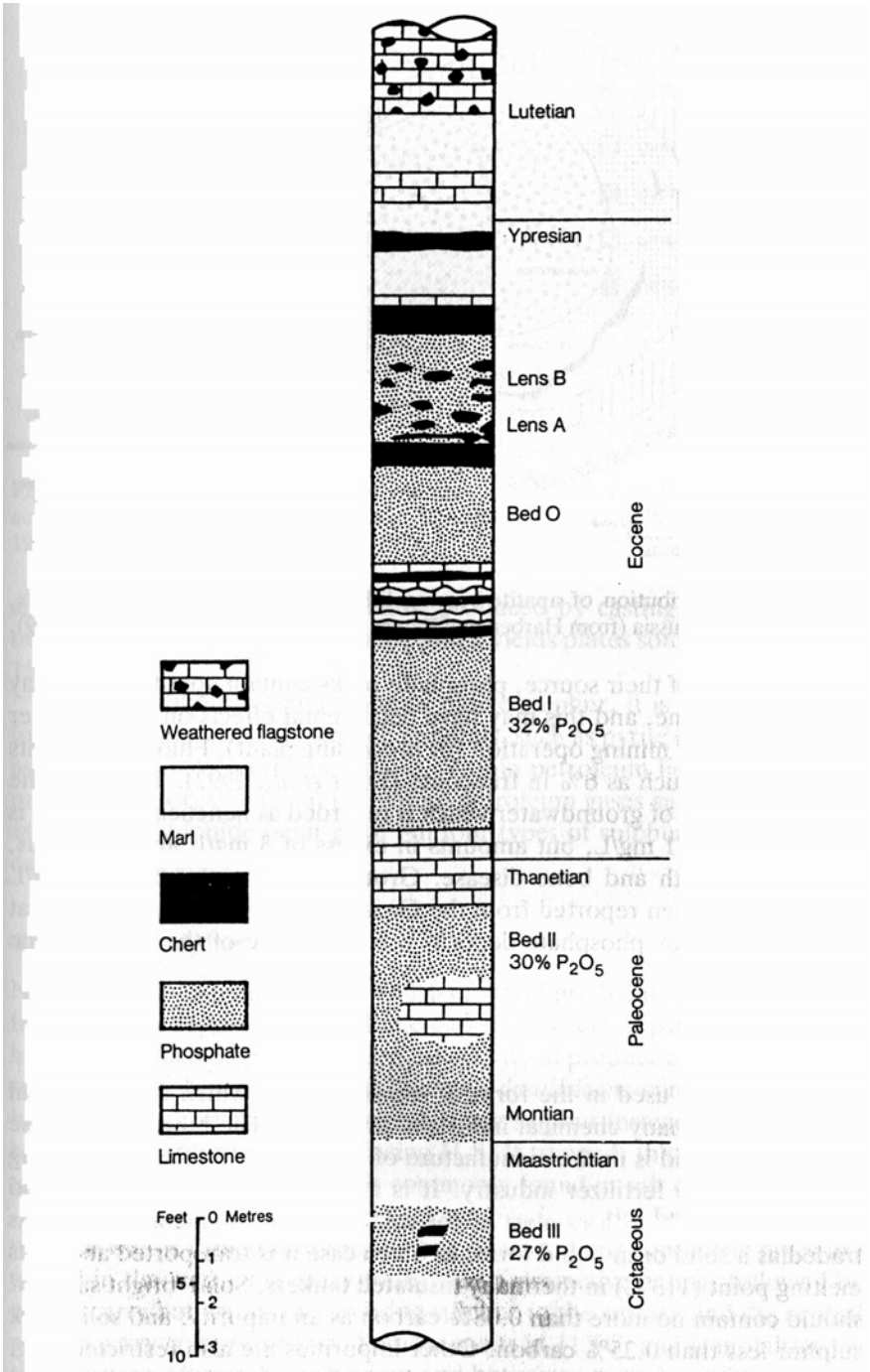

Figure 4.9 Representative vertical succession for the Khouribga phosphate deposit, Morocco (from Harben and Bates, 1990; adapted from Mew, 1980).

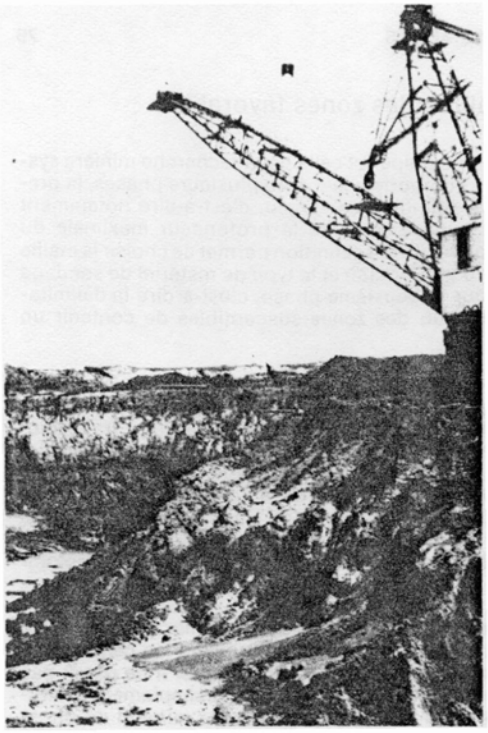

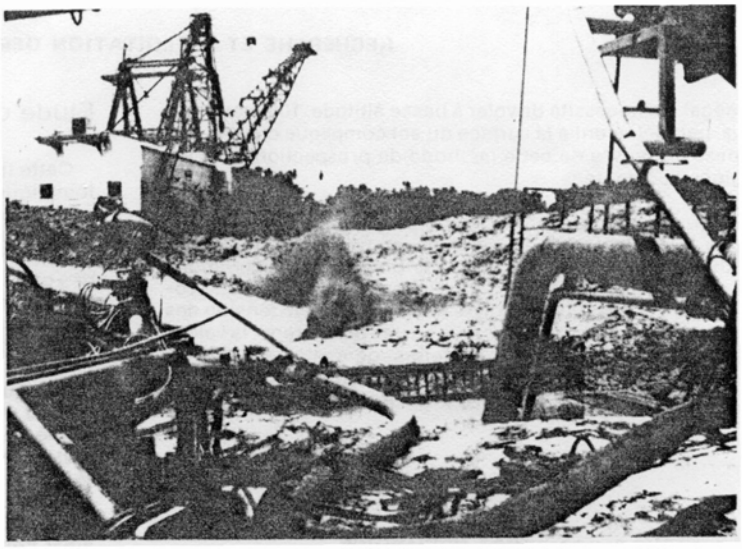

— **53** et **54.** Draglines utilisées en Floride. Ci-dessus : mise en pulpe du minerai pour son transport hydraulique à l'usine de traitement où le phosphate est séparé du quartz par flottation.

55. Camion de 100 t. utilisé à Taïba, Sénégal, pour le transport du tout-venant.

56. Draglines de l'exploitation de Taïba.

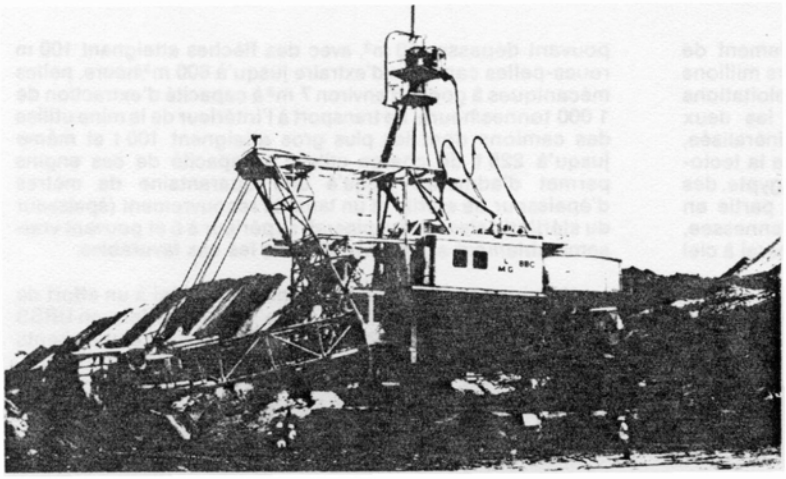

57. Roue-pelle utilisée dans le gisement du Togo pour enlever la couverture stérile.

M. Slansky (1980)

PRODUCCIÓN

www.iac.ac.in

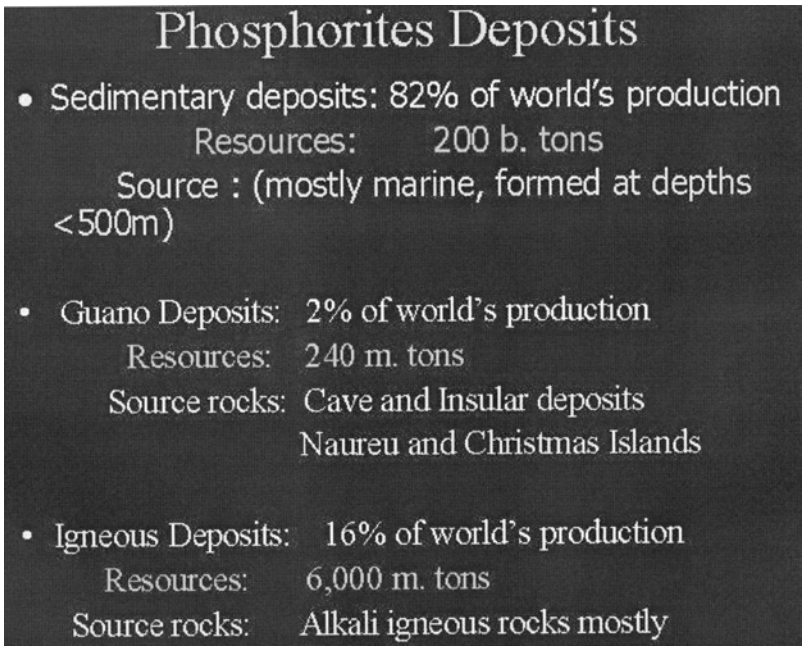

Table 128 Phosphate Rock: World Production

('000 tons gross weight)

	1990	1991	1992	1993	1994	1995
Algeria	1,128	1,090	1,136	718	738	757
Brazil	2,968	3,280	2,850	3,420	3,530	3,530
China	21,550	22,000	21,400	21,200	24,000	21,000
Egypt	1,143	1,652	2,000	1,585	1,500	1,500
Finland	546	472	555	628	647	671
Fomer USSR	36,800	28,400	X	X	X	X
India	674	610	488	969	1,176	1,250
Iraq	900	400	600	800	1,000	1,000
Israel	3,516	3,370	3,595	3,680	3,961	4,063
Jordan	6,082	4,433	4,296	4,129	4,217	4,984
Kazakhstan	X	X	7,000	4,000	2,000	2,200
Korea, North	500	550	500	510	510	520
Mexico	623	596	452	237	533	620
Morocco	21,396	17,900	19,145	18,193	19,764	20,200
Nauru	926	530	747	634	613	496
Russia	-	-	11,500	9,400	8,000	8,800
Senegal	2,147	1,741	2,284	1,670	1,670	1,600
South Africa	3,165	3,180	3,080	2,466	2,545	2,790
Syria	1,633	1,359	1,266	931	1,203	1,551
Togo	2,314	2,965	2,083	1,500	2,250	2,000
Tunisia	6,258	6,400	6,500	5,500	5,699	7,241
United States	46,343	48,096	46,965	35,494	41,100	43,500
Vietnam	274	274	275	363	470	480
Others	1,114	702	283	973	874	247
TOTAL	*162,000*	*150,000*	*139,000*	*119,000*	*128,000*	*131,000*

Source: USGS

Harben y Kuzvart (1996)

USOS

El término roca fosfatada se utiliza para cualquier roca que tiene menos del 18% de **pentóxido de fósforo P_2O_5** y fosforita aquella que tiene entre 18 y 40%. Para las leyes se utiliza tanto el contenido en P_2O_5 como el contenido en **fosfato tricálcico $Ca_3(PO_4)_2$ o fosfato de los huesos (BPL)**. El término BPL era utilizado cuando la principal fuente de fósforo eran los huesos de animales y humanos. Para hacer conversiones se utilizan las siguientes fórmulas: % P_2O_5 x 2,1853= %BPL; % P_2O_5 x 0,4364= %P y % BPL x 0,4576= % P_2O_5.

Cerca del **90% de los fosfatos** van para producir comercialmente **fertilizantes, sencillos o complejos,** junto con otros nutrientes primarios como el potasio, amonio y nitrógeno, y para ácido fosfórico (industria química). El fósforo es un nutriente indispensable para la vida pero es bastante insoluble y por ello deber ser convertido en forma de ortofosfato (H_2PO_4). Así, la roca fosfatada y fosforita conteniendo entre **5 y 30% de P_2O_5** se trata con ácido sulfúrico y se produce el **superfosfato normal o ácido fosfórico** procesado en húmedo H_3PO_4. Más tarde se transforma en ácido superfosfórico que es utilizado como punto de partida de muchos productos basados en fosfato. La roca fosfatada tratada con acido fosfórico se convierte en **trisuperfosfato o TSP** con **44 a 46% de P_2O_5** y es base para otros complejos utilizados en fertilizantes. También el TSP mezclado con amonio (CH_4) se produce el **mono-amonio-fosfato (MAP) y di-amonio-fosfato (DAP),** dos de los productos más ampliamente utilizados hoy día como fertilizantes. Si la roca fosfatada se utiliza con ácido nítrico se obtiene una variada de fertilizantes de **nitrofosfatos**, conteniendo entre 10 y 22 P_2O_5 ,y entre 14 y 22% de N. Los fertilizantes tienen tres número que significa la cantidad de N, P y K. Por ejemplo: 0-16-0 el superfosfato normal, 0-68-0 el ácido fosfórico, 11-48-0 el MAP o 18-46-0 el DAP.

El otro **10%** es consumido en una **gran variedad de industrias** incluyendo: detergentes, alimentos de animales, productos de bebida y comida, extintores del fuego, productos dentríficos y tratamiento superficial de metales. Si se combina el ácido fosfórico con sosa cáustica, Na(OH), se forma el fosfato de monosodio utilizado en el tratamiento de textiles, fotografía y productos de limpieza. La roca fosfatada y fosforita fundida con carbón y sílice da lugar a fósforo elemental P4, que se usa en bombas incendiarias, venenos, bengalas y productos pirotécnicos. Otros usos son: medicina, refinería de azúcar, etc.